Plant evolution further threatens declining pollinator populations

Avril Weinbach[1,2], Nicolas Loeuille[1], Rudolf P. Rohr[2]

1. Sorbonne Université, CNRS, Institut of Ecology and Environmental Sciences (iEES-Paris), place Jussieu, 75005, Paris, France;

2. Department of Biology, Ecology and Evolution, University of Fribourg, Switzerland.

Abstract

Recent pollinator population declines threaten pollination services and greatly impact plant-pollinator coevolution. In the present article, we investigate how such evolutionary effects affect plant-pollinator coexistence. Using eco-evolutionary dynamics, we study the evolution of plant attractiveness in a simple pollinator-plant model, assuming an allocation trade-off between attractiveness (e.g. nectar production, flower shape and size) and plant intrinsic growth rates. First, we investigated how attractiveness evolution changes species persistence, biomass production, and the intensity of the mutualism (as a proxy for pollination services). The shape of the allocation trade-off is key in determining the outcome of the eco-evolutionary dynamics. Only concave trade-offs allow convergence to stable plant-pollinator coexistence. Then we analyse the effect of pollinator population declines on the eco-evolutionary dynamics. Decreasing intrinsic growth rates of pollinator population results in a plant-evolution driven disappearance of the mutualistic interaction, eventually leading to pollinator extinction. With asymmetric mutualism favouring the pollinator, the evolutionary disappearance of the mutualistic interaction is delayed. Our results suggest that evolution may account for the current collapse of pollination systems and that restoration attempts should be enforced early enough to prevent potential negative effects driven by plant evolution.

Keywords: adaptive dynamics, plant attractiveness, pollinators decline, evolutionary murder, asymmetrical interactions, alternative stable states

1 Introduction

Recently observed severe declines in pollinator populations have been associated with that of insect-pollinated plants [1]. Understanding the future of pollinator and plant populations and proposing measures to mitigate this deterioration are essential given its strong impact on conservation and ecosystem services [2]. The global pollination crisis has been linked to habitat degradation, destruction, and fragmentation [3], but also to intensive agriculture, e.g. the use of herbicide and pesticides [4], overgrazing, and selective harvesting [5]. Increasing fire frequency [6], invasive animal and plant species [7], as well as diseases [8] are also natural threats to several pollinators. Finally, climate change is also predicted to have a strong impact on plant-pollinator interactions, as phenological shifts may weaken interactions between plants and pollinators [9].

Plants have been shown to adapt rapidly to changing pollinator populations [10–12]. A recent study from Gervasi and Schiestl [13] experimentally shown that changes in pollinator communities already affect plant trait evolution after only eleven generations. Exposed to bumblebees, which are very efficient pollinators, *Brassica rapa* plants evolved towards reinforcing attractiveness (e.g. traits attracting pollinators such as volatile organic compounds, flora size, or plant high). Hoverflies, which are less efficient pollinators, caused a 15-fold increase in self-reproduction and a reduction in plant attractiveness. Given these experimental results, the current deterioration and reshaping of pollinator communities may affect the evolution of plant species, which in turn could influence coexistence with their interacting pollinators.

Several theoretical studies have investigated the ecological [14–17] and evolutionary dynamics [18–22] of plant-pollinated communities. In particular, evolution of selfing with changing communities has been studied in several papers [23–25]. However, so far no study has investigated the consequence of declining pollinator populations on the eco-evolutionary process within a plant-pollinator community with evolving plant attractiveness. Here, we study this question in a system made of one plant species and one pollinator species. We investigate the evolution of plant attractiveness using an adaptive dynamics framework. This framework explicitly accounts for the eco-evolutionary feedback loop between the plant and the pollinator species. Using this model, we clarify when the plant species evolves to high or low attractiveness and determine the conditions under which evolution leads to coexistence of the whole system. We then show that a declining pollinator population often results in a counterselection of plant attractiveness, eventually enhancing pollinator declines.

2 Plant-pollinator model and ecological dynamics

We consider a simple system with two interacting species; a plant with population density P, and a pollinator with population density A. The community dynamics are given by a Lotka-Volterra type model:

$$\begin{cases} \frac{dA}{dt} = N\left(r_A - c_A A + \alpha \gamma_P P\right) \\ \frac{dP}{dt} = P\left(r_P - c_P P + \alpha \gamma_A A\right) \end{cases} \tag{1}$$

A schematic view of the system is given in figure 1. The parameters r_A and r_P correspond to the intrinsic growth rate of the pollinator and plant species, respectively. We assume r_P to be strictly positive because of other reproduction means, e.g. vegetative reproduction or

autogamy. The intrinsic growth rate of the pollinator (r_A) can be positive (e.g., interaction with other plants) or negative. Parameters c_A and c_P modulates intraspecific competition for the two species. Mutualistic interactions are given by $\alpha \gamma_A$ and $\alpha \gamma_P$, with γ_P the energetic gain provided by the plant (via nectar, pollen and/or other plant exudates) to the pollinator, and γ_A the fertilisation provided by the pollinator to the plant. Parameter α represents the plant attractiveness, largely defined and corresponds to the trait that will be under selection in the rest of the study. This attractiveness includes investment in various characters such as the number of flowers, their shape, their colour, volatile organic compound (VOCs) that attract insects with their odor, plant height, flowering duration (see part II in Willmer (2011) [26]).

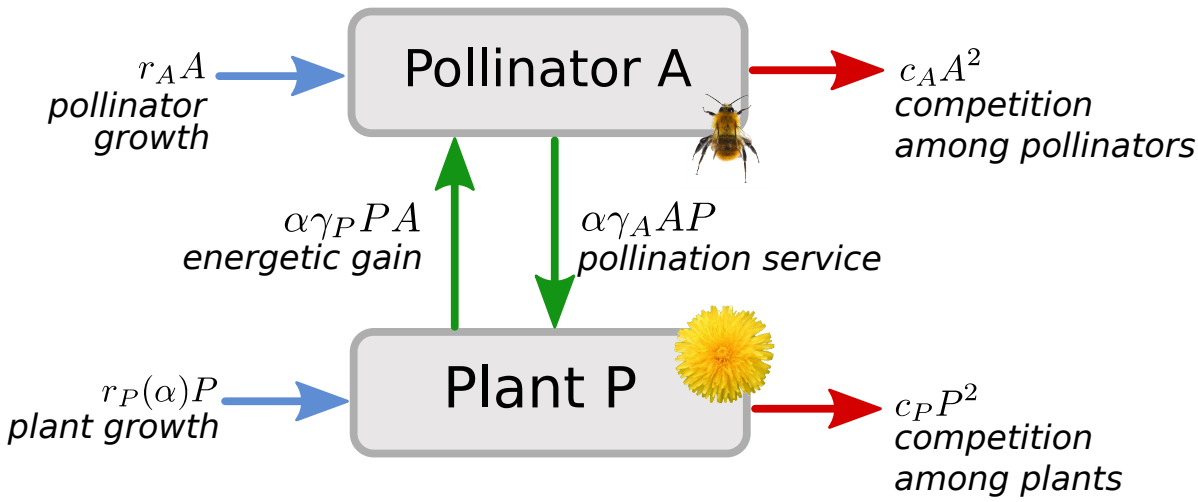

Figure 1: ***Population variation rates of plant*** P ***and pollinator*** A ***.*** *Blue arrows indicate the density variations independent of the mutualistic interaction, green arrows the effects of the mutualistic interaction, and red arrows the effects of intraspecific competition. The parameters are described in the main text.*

The ecological dynamics of equivalent models were studied by Goh (1979) [14]. Extrapolating from his results, coexistence of the two species in time can be maintained provided:

$$\begin{cases} \dfrac{\alpha \gamma_P r_P + c_P r_A}{c_A c_P - \alpha^2 \gamma_A \gamma_P} > 0 \\ \dfrac{\alpha \gamma_A r_A + c_A r_P}{c_A c_P - \alpha^2 \gamma_A \gamma_P} > 0 \\ \alpha^2 \gamma_A \gamma_P < c_A c_P \end{cases} \tag{2}$$

The first two inequalities give the condition for the existence of an equilibrium point allowing positive densities (feasibility conditions). The last inequality ensures the dynamical stability of the equilibrium. In the case of two interacting species, this local stability condition implies the global stability of the feasible equilibrium. The globally stable equilibrium is then:

$$\begin{cases} A^* = \dfrac{\alpha \gamma_P r_P + c_P r_A}{c_A c_P - \alpha^2 \gamma_A \gamma_P} \\ P^* = \dfrac{\alpha \gamma_A r_A + \alpha_A r_P}{c_A c_P - \alpha^2 \gamma_A \gamma_P} \end{cases} \tag{3}$$

If the stability condition is not fulfilled, i.e., interspecific mutualism is stronger than intraspecific competition, the positive feedback loop resulting from interspecific mutualism may drive the system towards infinite growth. In such cases, other limiting factors (e.g. pathogen, predators, or new competitors) eventually regulate the populations. Since these factors are not taken into account in our model assumptions, we define a maximum plant attractiveness α_{cl} below which stability is warranted:

$$\alpha_{cl} = \sqrt{\frac{c_A c_P}{\gamma_A \gamma_P}}. \tag{4}$$

We allow the evolution of α between zero (no investment in attractiveness) and this maximal level $\alpha_{max} < \alpha_{cl}$.

3 Evolution of plant attractiveness

We study the evolution of plant attractiveness (α), assuming an allocation trade-off affecting r_P [27]. The plant has a given quantity of energy, divided into different functions; some

energy is allocated to intrinsic growth and to self-reproduction, and some to attractiveness [27,28]. We consider different trade-off shapes; linear, concave or convex. The shape of the trade-off is controlled by the parameter s ($s>1$ concave; $s=1$ linear; $s<1$ convex). Detailed mathematical formulations of the trade-off functions are given in the supplementary material.

We follow the evolution of plant attractiveness using adaptive dynamics. This method models explicitly the evolutionary consequences on species density dynamics, and the feedback of species density on the evolutionary process [29,30]. Evolution occurs via small mutations steps between which densities reach the ecological equilibrium. It also assumes clonal reproduction and small phenotypic impact of the mutations. The differential equation describing the evolution of the phenotypic traits, known as the canonical equation [29], is given by:

$$\frac{d\alpha}{dt}=\frac{1}{2}\mu\sigma^2 P^*(\alpha)\left.\frac{\partial\omega(\alpha_m,\alpha)}{\partial\alpha_m}\right|_{\alpha_m\to\alpha} \tag{5}$$

The term $\frac{1}{2}\mu\sigma^2 P^*(\alpha)$ encapsulates the phenotypic variability brought by the mutation process on which selection can act; with μ the per individual mutation rate, σ^2 the variance of the mutation phenotypic effect, and $P^*(\alpha)$ the plant equilibrium density. The last term is called the selective gradient. It embodies the effects of natural selection, based on the variations of the relative fitness of mutants α_m given a resident population of attractiveness α. Therefore, the sign of the selective gradient gives the direction of evolution; a positive gradient selects larger attractiveness, while a negative gradient selects smaller trait values. The relative fitness of a mutant at a very low density is explicitly derived from the ecological dynamics (equation (1)). It is computed as the *per capita* growth rate of a rare mutant population in a resident population at ecological equilibrium (3):

$$\omega(\alpha_m,\alpha)=\frac{1}{P_m}\frac{dP_m}{dt}\bigg|_{P_m\to 0}=r_P(\alpha_m)-c_P P^*(\alpha)+\alpha_m \gamma_A A^*(\alpha), \tag{6}$$

with $P^*(\alpha)$ and $A^*(\alpha)$ given by equation 3. Remember that, due to the allocation costs, the plant intrinsic growth rate varies with the level of attractiveness $r_P(\alpha)$.

Eco-evolutionary dynamic (equation 5) may exhibit equilibrium points, called evolutionary singular strategies. They correspond to trait values at which the adaptive dynamic (5) is at equilibrium, i.e., the time derivative is equal to zeros. Since all terms apart the selective gradient are always positive, the singular strategies occur when the selective gradient is null. This corresponds to values $\hat{\alpha}$ satisfying:

$$\frac{\partial\omega(\alpha_m,\alpha)}{\partial\alpha_m}\bigg|_{\alpha_m,\alpha\to\hat{\alpha}}=\frac{dr_P(\hat{\alpha})}{d\hat{\alpha}}+\gamma_A A^*(\hat{\alpha})=0. \tag{7}$$

At singularities, costs in terms of energy dedicated to alternative means of reproduction ($dr_P(\hat{\alpha})/d\hat{\alpha}$) therefore match pollination benefits ($\gamma_A A^*(\hat{\alpha})$). The existence of a singular strategy is not enough to guarantee that evolutionary dynamics locally lead to it (convergence condition) or that it persists (non-invasibility condition, i.e. resistance to invasion by nearby mutants). A singular strategy that is both convergent and non-invasible is called a continuously stable strategy (CSS) [31]. To have long-term coexistence, the evolutionary process needs to converge to a CSS at which we have ecological coexistence of the plant and the pollinator. Three other types of singular strategies can arise from the evolutionary process: Garden of Eden (non-convergent and non-invasible), repellor (non-convergent and invasible), and branching points (convergent and invasible). Calculation of the second and cross-derivative of the fitness function determines criteria for convergence and invasibility [32]. The mathematical computation for the existence of singular strategies and their convergence and invasibility properties are given in the supplementary material.

Equation (7) can be solved analytically for particular set of parameters (see supplementary material). For other cases, we graphically determine the values and the convergence and invasibility properties of the singular strategies using the pairwise invasibility plots (figure 2). Figure 2 illustrates the singular strategies and their properties depending on the trade-off shape and the pollinator intrinsic growth rate. It is possible to show (supplementary material), as illustrated in figure 2, that only concave allocative trade-offs lead to non-invasible strategies. Therefore, long-term coexistence needs a concave trade-off function. Then, the convergence to a singular strategy depends on the pollinator intrinsic growth rate (figure 2c and 2d). While analytical calculation was intractable for the convergence condition, except with the linear case for which we always obtain a divergent singular strategy, we could explore the model using sensitivity analysis and the PIPs. For positive pollinator intrinsic growth rate, we obtain only one convergent stable singular strategies (CSS) at which the ecological coexistence is granted. In that case, long-term coexistence is obtained. For negative pollinator intrinsic growth rate, the system exhibits a second singular strategy that is a Garden of Eden. In the following, we will study only concave trade-off function (i.e. $s>1$).

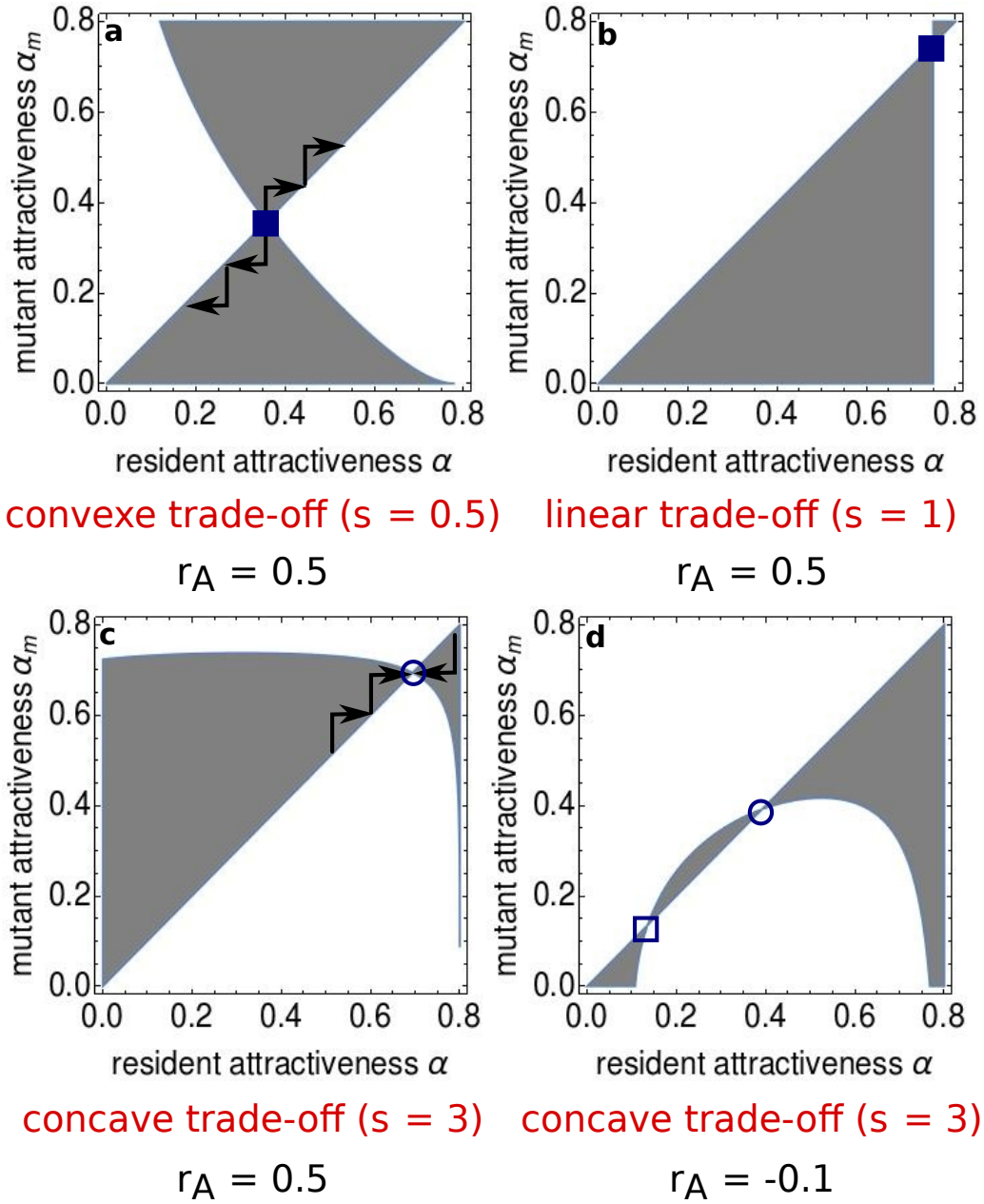

Figure 2*: **Pairwise invasibility plots (PIPs) representing the invasibility potential of a rare mutant** α_m **within a resident plant population** α **at ecological equilibrium.** Grey areas indicates that the mutant relative fitness* $\omega(\alpha_m, \alpha)$ *is positive so that it invades and replaces the resident population. In panels a and c, arrows show the direction of evolutionary trajectories. The system exhibits several singular strategies depending on the parameter values. Circles represent convergent strategies, whereas squares are non-convergent. Filled symbols represent invasible strategy, while not filled symbols are non-invasible. In panel a and b, the singular strategy is non-convergent and invasible (repellor). In panel c, the singular strategy is convergent and non-invasible (CSS). Panel d displays two strategies, one CSS and one which is non-convergent and non-invasible (Garden of Eden). Parameter values are:* $c_A = c_P = \gamma_A = \gamma_P = 1$ *, and* $\alpha_{max} = 0.8 * \alpha_{cl}$ *.*

4 Consequences of pollinator population decline

Now that we have characterised the plant evolutionary dynamics, we show how pollinator decline may affect the outcome. We assume that pollinators suffer less favourable environmental conditions (e.g. habitat fragmentation, pesticides, diseases) so that their intrinsic growth rate (r_A) is decreased. We illustrate the effects of this disturbance through Ecology-Evolution-Environment (E^3) diagrams [33,34]. These diagrams show the outcome of eco-evolutionary dynamics as function of the environmental parameter. Figure 3 represents such a diagram for the same concave-trade off and parameters values (except for variations in pollinator intrinsic growth rate) of figure 2c,d. The X-axis of the diagram represents the environment (intrinsic growth rate: r_A). The Y-axis represents the evolving trait value relative to its maximum value (attractiveness ratio: $\frac{\alpha}{\alpha_{max}}$). The colour illustrates variations in equilibrium densities for the pollinator (panel a) and the plant (panel b): white represents extinction, while the intensity of blue gradient correlates with species densities. This E^3 diagram exhibits two types of singular strategies: a convergent and stable singular strategy (CSS, continuous line), and Garden of Eden (dotted line). The vertical black arrows give the direction of evolution. The Garden of Eden singular strategy is present only for negative pollinator intrinsic growth rates, which can be considered as a bad environment for the pollinator. In this case, the system exhibits evolutionary alternative stable states; for a plant attractiveness above the Garden of Eden value the evolution converge toward the CSS, while for a plant attractiveness below, selection leads to ever-decreasing attractiveness, weakening the mutualistic interaction and eventually leading to the extinction of the pollinator (arrow (7) in figure 3a).

For positive pollinator intrinsic growth rates ($r_A > 0$), the system converges toward a CSS

with intermediate α (arrows (1) and (2) in figure 3a). Now consider the environmental degradation (red arrow (3) in figure 3a). At this point, in the absence of evolution, both plant and pollinator populations are maintained at positive densities. However, considering evolution, plant attractiveness decreases as pollinators being too rare to compensate the intrinsic costs of attractiveness. Eventually, evolution drives pollinator populations to extinction; an evolutionary murder depicted by arrow (4) in figure 3a. Faced with the crash of pollinator populations, restoration plans may be undertaken. Early intervention, depicted by arrow (5), can restore a coexisting system. Yet, a delayed restoration (white arrow (6)), will not allow such a rescue, as evolutionary trajectories diverge from the Garden of Eden singularity eventually leading to the extinction of the pollinator (arrow (7)).

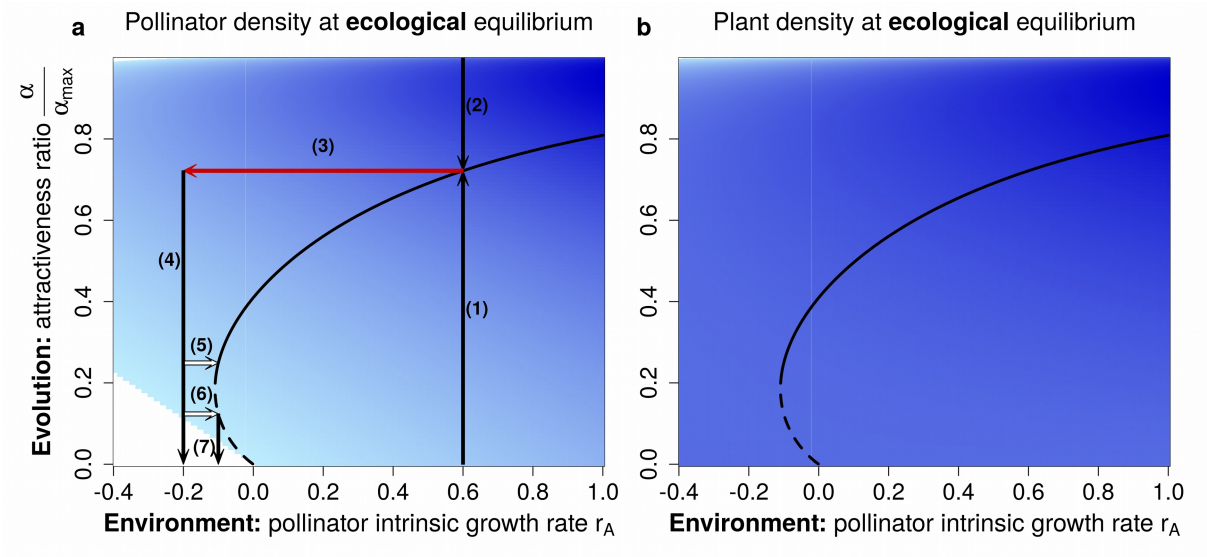

Figure 3: ***Ecology-evolution-environment (E^3) diagram representing the impact of the environment on the evolution of plant attractiveness and on pollinator (panel a) and plant equilibrium densities (panel b).*** *White areas show parameters for which extinction occurs for either plants or pollinators. . The blue intensity correlates with population densities of pollinators (panel a) or plants (panel b). Black lines show the position of singular strategies; continuous lines show convergent and non-invasible singular strategies (CSS) , and dashed lines show Garden of Edens (non-invasible, divergent). Vertical black arrows (1, 2, 4, 7) give the direction of evolution. Environmental disturbance is represented by a red arrow (3). White arrows (5, 6) represent restoration attempts at different times along the evolutionary trajectory .Parameters values are* $s=2.5$, $c_A=c_P=\gamma_P=1$, $\gamma_A=0.2$ *, and* $\alpha_{max}=0.8*\alpha_{cl}$.

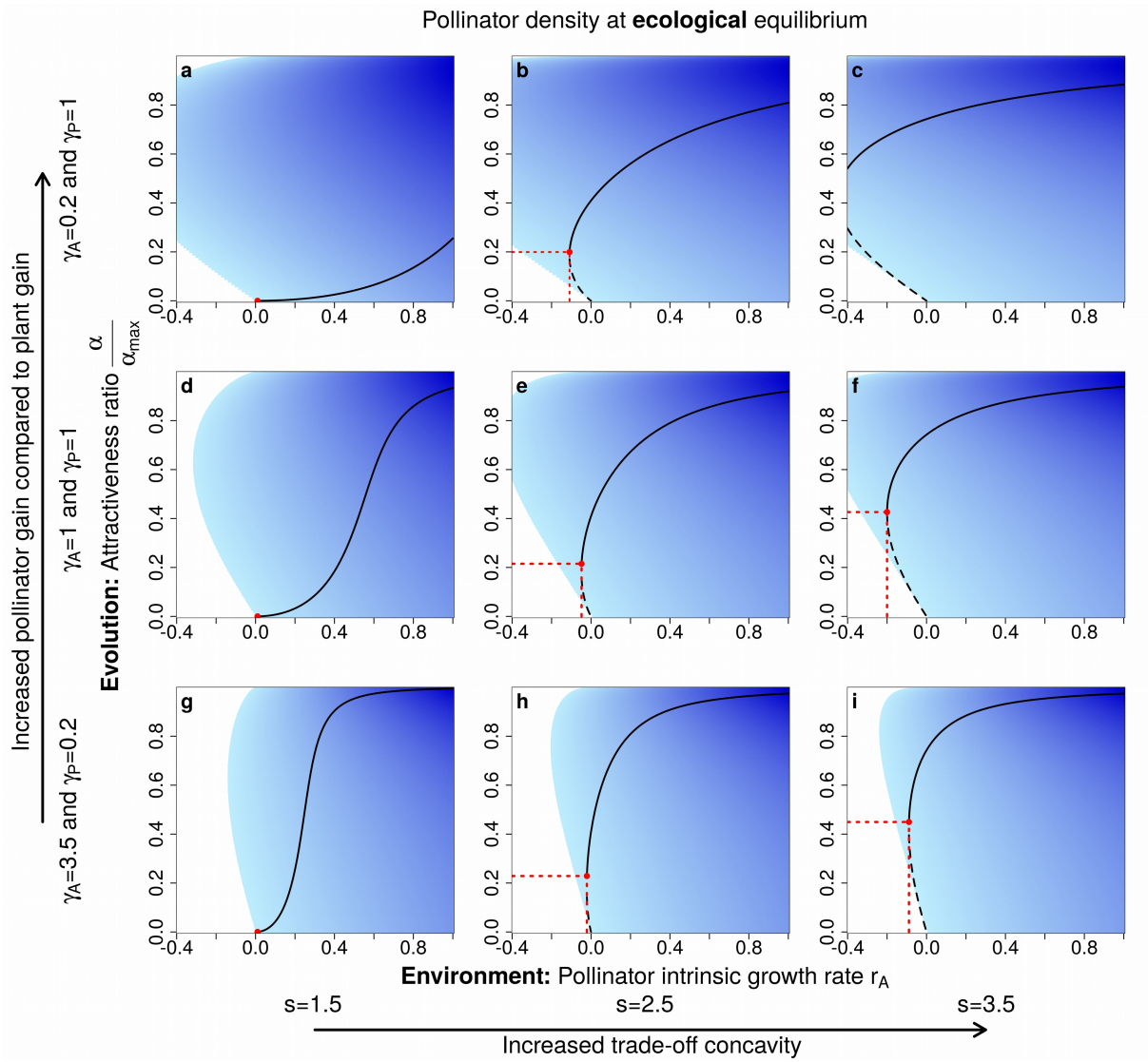

Figure 4: ***Influence of trade-off shape and mutualistic gains on*** E^3 ***diagrams.*** *Columns differ in trade-off concavity. More concave trade-offs allow a larger coexistence domain. Lines of panels differ in the asymmetry of mutualistic gains: in the top line (panels a,b , and c) pollinators benefits more than plants; the middle line (panels d,e, and f) shows equal gains while in the bottom line plant gains are larger. The red points anddotted lines represent the lowest* r_A *and* $\frac{\alpha}{\alpha_{max}}$ *values for maintaining a CSS, leading to ecological and evolutionary coexistence. Asymmetry in favour of the pollinator or more concave trade-offs allow a larger domain for eco-evolutionary coexistence. Colours and lines are the same as in figure 3. The parameter values are* $c_A = c_P = 1$ *and* $\alpha_{max} = 0.8 * \alpha_{cl}$ *.*

Finally, we study the impact of trade-off shapes and of the asymmetry between mutualistic gains on the eco-evolutionary outcome (figure 4). For strong concave trade-offs, s > 2, (figure 4b, c, e, f, h, i) we observe qualitatively the same dynamics as in figure 3. For less concave

trade-offs, s < 2, only a positive pollinator intrinsic growth rate r_A allows coexistence (figure 4a,d,g). In this case, negative pollinator intrinsic growth rates lead to small benefits of the mutualistic interaction for the plant, so that attractiveness is counterselected, eventually leading to the pollinator extinction [35]. For more concave trade-offs (s > 2), we notice that an asymmetric mutualistic gain favouring pollinators allows a larger range, including negative intrinsic growth rates r_A, before attractiveness is counterselected and extinction occurs. Therefore, an increased mutualistic gain of the pollinator relative to that of plant facilitates the long term coexistence of the plant-pollinated system. This produces a more robust system that eases a potential restoration process. Note, however, that favouring pollinators gain over plants leads lower selected levels of attractiveness.

5 Discussion

The present work highlights how evolution may play a critical role for mutualistic interaction maintenance in time. We especially show that evolution may actually be detrimental to this persistence. While we studied a simple two species plant-pollinator system, this allows us to mathematically study the eco-evolutionary dynamics and completely investigate the role of key parameters (e.g. trade-off shapes or mutualistic gains). We showed that only concave trade-offs can lead to stable coexistence in evolutionary times (figure 2). Then we investigated the impact of environmental disturbances simulating the decrease of pollinator intrinsic growth rates (figures 3 and 4). We show that only strong concave trade-offs (s > 2) allow coexistence in degraded environments. Interestingly, the system then exhibits alternative (evolutionary) stable states: a CSS at which the plant and the pollinator coexist, and selection toward ever-decreasing attractiveness, eventually leading to the pollinator extinction (ie, an evolutionary murder of the pollinator by the plant). These two states are

separated by a (divergent) Garden-of-Eden evolutionary singular strategy. This is an example of critical transition of a stable and convergent evolutionary strategy, for positive pollinator intrinsic growth rate, to evolutionary bistability for negative pollinator intrinsic growth rate.

Bistability has been highlighted in a variety of ecological situations (e.g. [36], [37] in mutualistic system), and results from a strong positive ecological feedback loop.

Above a critical value, the system will amplify toward a stable state with higher values, but below, the system will shift to an alternative, degraded, stable state. Here we have a similar phenomenon, but on an eco-evolutionary scale. If plant attractiveness before pollinator deterioration is above the level of the Garden of Eden singular strategy, plant evolution reinforces its attractiveness toward higher values eventually reaching a stable, coexisting system (CSS). On an ecological scale, the interaction reinforcement increases the abundance of both plants and pollinators, which in turn favours the evolution of plant attractiveness toward higher value. Below the critical level, evolution decreases plant attractiveness, which in turn decreases pollinator abundance that feedback into an evolutionary decrease of plant attractiveness. This feedback eventually leads to the evolutionary murder of the pollinator by the plant [35]. Note that the trade-off shape modulates the strength of the positive feedback loop. More concave trade-offs decrease the threshold value above which the positive feedback loop is maintained, thereby facilitating the persistence of the system.

On a management side, alternative stable states have large implications, as systems may then shift abruptly, and large restorations are needed to recover previous states [36]. The eco-evolutionary alternative stable states we describe here have similar implications. Our results show that they make restoration attempts more difficult from two different points of view. First, as highlighted in figure 3, the timing of the attempt becomes important. Restoration is only successful when achieved before the threshold attractiveness is evolved (see figure 3).

Second, just as in ecological hysteresis, if the system becomes degraded, a small restoration attempt will not be sufficient to recover large populations, but large efforts will have to be undertaken.

These results are consistent with the experiment of Gervasi and Schiestl [13]. . A decrease in efficient pollinators indeed leads to less investment in sexual reproduction and attractiveness from the plant side with an increase in selfing (the reproductive assurance hypothesis). This trend is consistent with other empirical observations (e.g. [41]). Our results question the efficiency of restoration policies that would solely focus on ecological or environmental restoration. Indeed, here, plant evolution hinder restoration attempts that would have been successful if just ecological dynamics had been considered. Whether evolution indeed weakens or threaten plant-pollinator interactions in the face of external disturbances needs further investigation to properly understand the current pollination crisis (e.g. [42] on plant decline but questioned in [43]).

6 Bibliography

1. Biesmeijer JC *et al.* 2006 Parallel Declines in Pollinators and Insect-Pollinated Plants in Britain and the Netherlands. *Science* **313**, 351–354. (doi:10.1126/science.1127863)

2. Klein A-M, Vaissière BE, Cane JH, Steffan-Dewenter I, Cunningham SA, Kremen C, Tscharntke T. 2007 Importance of pollinators in changing landscapes for world crops. *Proc. R. Soc. Lond. B Biol. Sci.* **274**, 303–313. (doi:10.1098/rspb.2006.3721)

3. Steffan-Dewenter I, Klein A-M, Gaebele V, Alfert T, Tscharntke T. 2006 Bee diversity and plant-pollinator interactions in fragmented landscapes. *Spec. Gen. Plant-Pollinator Interact.* , 387–410.

4. Kevan PG. 1975 Forest application of the insecticide fenitrothion and its effect on wild bee pollinators (Hymenoptera: Apoidea) of lowbush blueberries (Vaccinium SPP.) in Southern New Brunswick, Canada. *Biol. Conserv.* **7**, 301–309. (doi:10.1016/0006-3207(75)90045-2)

5. Aizen MA, Vazquez DP. 2006 Flower performance in human-altered habitats. In *In The Ecology and Evolution of Flowers*, pp. 159–179.

6. Potts SG, Vulliamy B, Dafni A, Ne'eman G, O'Toole C, Roberts S, Willmer P. 2003 Response of plant-pollinator communities to fire: changes in diversity, abundance and floral reward structure. *Oikos* **101**, 103–112. (doi:10.1034/j.1600-0706.2003.12186.x)

7. Madjidian JA, Morales CL, Smith HG. 2008 Displacement of a native by an alien bumblebee: lower pollinator efficiency overcome by overwhelmingly higher visitation frequency. *Oecologia* **156**, 835–845. (doi:10.1007/s00442-008-1039-5)

8. Conte YL, Ellis M, Ritter W. 2010 Varroa mites and honey bee health: can Varroa explain part of the colony losses? *Apidologie* **41**, 353–363. (doi:10.1051/apido/2010017)

9. Parmesan C. 2006 Ecological and Evolutionary Responses to Recent Climate Change. *Annu. Rev. Ecol. Evol. Syst.* **37**, 637–669. (doi:10.1146/annurev.ecolsys.37.091305.110100)

10. Darwin C. 1877 *On the various contrivances by which British and foreign orchids are fertilised by insects*.

11. Hopkins R, Rausher MD. 2012 Pollinator-Mediated Selection on Flower Color Allele Drives Reinforcement. *Science* **335**, 1090–1092. (doi:10.1126/science.1215198)

12. van der Niet T van der, Johnson SD. 2012 Phylogenetic evidence for pollinator-driven diversification of angiosperms. *Trends Ecol. Evol.* **27**, 353–361. (doi:10.1016/j.tree.2012.02.002)

13. Gervasi DDL, Schiestl FP. 2017 Real-time divergent evolution in plants driven by pollinators. *Nat. Commun.* **8**, 14691. (doi:10.1038/ncomms14691)

14. Goh BS. 1979 Stability in Models of Mutualism. *Am. Nat.* **113**, 261–275.

15. Thébault E, Fontaine C. 2010 Stability of Ecological Communities and the Architecture of Mutualistic and Trophic Networks. *Science* **329**, 853–856. (doi:10.1126/science.1188321)

16. Rohr RP, Saavedra S, Bascompte J. 2014 On the structural stability of mutualistic systems. *Science* **345**, 1253497. (doi:10.1126/science.1253497)

17. Saavedra S, Rohr RP, Olesen JM, Bascompte J. 2016 Nested species interactions promote feasibility over stability during the assembly of a pollinator community. *Ecol. Evol.* **6**, 997–1007. (doi:10.1002/ece3.1930)

18. Ferriere R, Bronstein JL, Rinaldi S, Law R, Gauduchon M. 2002 Cheating and the evolutionary stability of mutualisms. *Proc. R. Soc. Lond. B Biol. Sci.* **269**, 773–780. (doi:10.1098/rspb.2001.1900)

19. De Mazancourt C, Schwartz MW. 2010 A resource ratio theory of cooperation. *Ecol. Lett.* **13**, 349–359. (doi:10.1111/j.1461-0248.2009.01431.x)

20. Toby Kiers E, Palmer TM, Ives AR, Bruno JF, Bronstein JL. 2010 Mutualisms in a changing world: an evolutionary perspective. *Ecol. Lett.* **13**, 1459–1474. (doi:10.1111/j.1461-0248.2010.01538.x)

21. Georgelin E, Loeuille N. 2016 Evolutionary response of plant interaction traits to nutrient

enrichment modifies the assembly and structure of antagonistic-mutualistic communities. *J. Ecol.* **104**, 193–205. (doi:10.1111/1365-2745.12485)

22. Valdovinos FS, Brosi BJ, Briggs HM, Moisset de Espanés P, Ramos-Jiliberto R, Martinez ND. 2016 Niche partitioning due to adaptive foraging reverses effects of nestedness and connectance on pollination network stability. *Ecol. Lett.* **19**, 1277–1286. (doi:10.1111/ele.12664)

23. Cheptou P, Massol F. 2009 Pollination Fluctuations Drive Evolutionary Syndromes Linking Dispersal and Mating System. *Am. Nat.* **174**, 46–55. (doi:10.1086/599303)

24. Lepers C, Dufay M, Billiard S. 2014 How does pollination mutualism affect the evolution of prior self-fertilization? A model. *Evolution* **68**, 3581–3598. (doi:10.1111/evo.12533)

25. Astegiano J, Massol F, Vidal MM, Cheptou P-O, Jr PRG. 2015 The Robustness of Plant-Pollinator Assemblages: Linking Plant Interaction Patterns and Sensitivity to Pollinator Loss. *PLOS ONE* **10**, e0117243. (doi:10.1371/journal.pone.0117243)

26. Willmer P. 2011 *Pollination and Floral Ecology*. Princeton University Press.

27. Willmer P. 2011 Rewards and costs: the environmental economics of pollination. In *Pollination and Floral Ecology*, pp. 234–257. Princeton University Press.

28. Obeso JR. 2002 The costs of reproduction in plants. *New Phytol.* **155**, 321–348. (doi:10.1046/j.1469-8137.2002.00477.x)

29. Dieckmann U, Law R. 1996 The dynamical theory of coevolution: a derivation from stochastic ecological processes. *J. Math. Biol.* **34**, 579–612. (doi:10.1007/BF02409751)

30. Geritz S a. H, Kisdi E, Mesze NA G, Metz J a. J. 1998 Evolutionarily singular strategies and the adaptive growth and branching of the evolutionary tree. *Evol. Ecol.* **12**, 35–57. (doi:10.1023/A:1006554906681)

31. Christiansen FB. 1991 On Conditions for Evolutionary Stability for a Continuously Varying Character. *Am. Nat.* **138**, 37–50.

32. Marrow P, Dieckmann U, Law R. 1996 Evolutionary dynamics of predator-prey systems: an ecological perspective. *J. Math. Biol.* **34**, 556–578. (doi:10.1007/BF02409750)

33. Dieckmann U, Ferrière R. 2004 Adaptive dynamics and evolving biodiversity. In *Evolutionary conservation biology*, pp. 188–224. Cambridge: Cambridge University Press.

34. Ferriere R, Legendre S. 2013 Eco-evolutionary feedbacks, adaptive dynamics and evolutionary rescue theory. *Phil Trans R Soc B* **368**, 20120081. (doi:10.1098/rstb.2012.0081)

35. Dercole F, Ferriere R, Rinaldi S. 2002 Ecological Bistability and Evolutionary Reversals Under Asymmetrical Competition. *Evolution* **56**, 1081–1090. (doi:10.1111/j.0014-3820.2002.tb01422.x)

36. Scheffer M, Carpenter SR. 2003 Catastrophic regime shifts in ecosystems: linking theory to observation. *Trends Ecol. Evol.* **18**, 648–656. (doi:10.1016/j.tree.2003.09.002)

37. Hairston NG, Ellner SP, Geber MA, Yoshida T, Fox JA. 2005 Rapid evolution and the convergence of ecological and evolutionary time. *Ecol. Lett.* **8**, 1114–1127. (doi:10.1111/j.1461-0248.2005.00812.x)

38. Roels SAB, Kelly JK. 2011 Rapid Evolution Caused by Pollinator Loss in Mimulus Guttatus. *Evolution* **65**, 2541–2552. (doi:10.1111/j.1558-5646.2011.01326.x)

39. Bascompte J, Jordano P, Olesen JM. 2006 Asymmetric Coevolutionary Networks Facilitate Biodiversity Maintenance. *Science* **312**, 431–433. (doi:10.1126/science.1123412)

40. Wang R-W, Sun B-F, Zheng Q, Shi L, Zhu L. 2011 Asymmetric interaction and indeterminate fitness correlation between cooperative partners in the fig–fig wasp mutualism. *J. R. Soc. Interface* **8**, 1487–1496. (doi:10.1098/rsif.2011.0063)

41. Devaux C, Lepers C, Porcher E. 2014 Constraints imposed by pollinator behaviour on the ecology and evolution of plant mating systems. *J. Evol. Biol.* **27**, 1413–1430. (doi:10.1111/jeb.12380)

42. Bond WJ. 1994 Do Mutualisms Matter? Assessing the Impact of Pollinator and Disperser Disruption on Plant Extinction. *Philos. Trans. R. Soc. Lond. B Biol. Sci.* **344**, 83–90. (doi:10.1098/rstb.1994.0055)

43. Frederickson ME. 2017 Mutualisms Are Not on the Verge of Breakdown. *Trends Ecol. Evol.* **32**, 727–734. (doi:10.1016/j.tree.2017.07.001)

Electronic Supplementary material

The allocation trade-off

Evolution acts on the plant attractiveness α, that we assume constrained by an allocation trade-off to the plant intrinsic growth rate r_P [1]. The plant has a given quantity of energy, divided into different functions: some energy is allocated to intrinsic growth and reproduction, and some to attractiveness [2]. That is why we model r_P as a decreasing function of the attractiveness α:

$$\left(\frac{r_P}{r_{Pmax}}\right)^s + \left(\frac{\alpha}{\alpha_{max}}\right)^s = 1. \qquad \text{(A1)}$$

The plant maximal intrinsic growth rate r_{Pmax} can be fixed to one without loss of generality, by choosing appropriately the time unit. Using (A1) we can express the plant intrinsic growth rate depending on the plant attractiveness:

$$r_P = \left(1 - \left(\frac{\alpha}{\alpha_{max}}\right)^s\right)^{1/s}. \qquad \text{(A2)}$$

The s exponent controls the trade-off shape. When $s=1$ there is a linear relationship between r_P and α. When $0<s<1$ the trade-off is convex. On the opposite, $s>1$ will produce a concave trade-off. Examples of the trade-off variations can be found in figure 1.

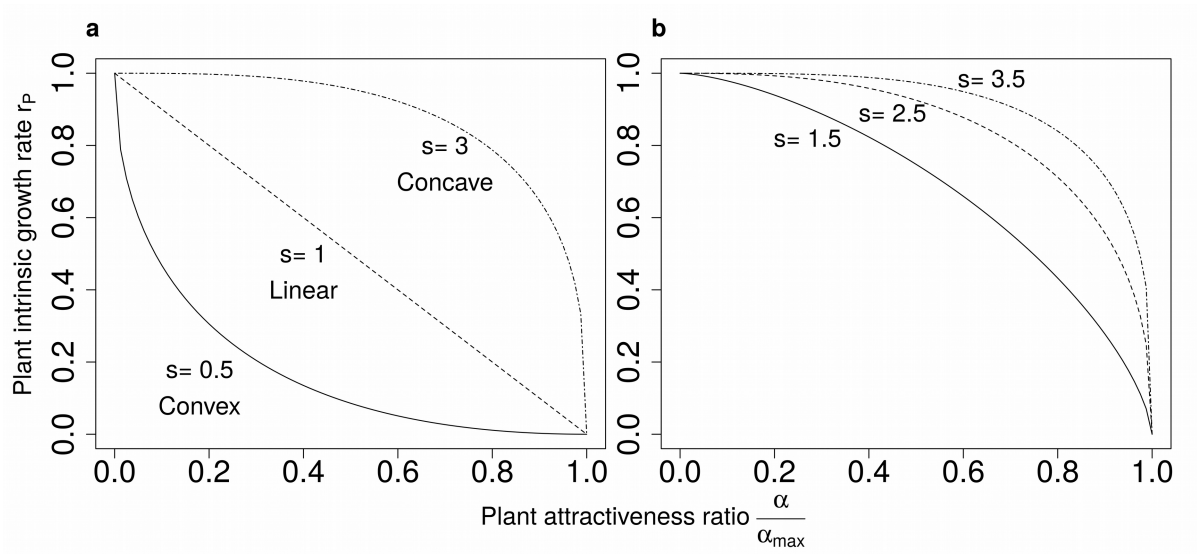

Figure 1*: **Variation of the attractiveness ratio** $\frac{\alpha}{\alpha_{max}}$ **with the plant intrinsic growth rate** r_P **depending on the trade-off strength**. On panel a, The continuous line represents a convex trade-off, the dashed line a linear trade-off, and the dashed-dotted line a concave trade-off. On panel b we represented different curvatures of a concave trade-off function, depending on the value of the parameter s.*

Detailed eco-evolutionary dynamics

Detailed analysis of singular strategies

In this part the symbol $*$ signal the ecological equilibrium and $\hat{\square}$ the evolutionary one.

The evolving variable α impact the plant intrinsic growth rate r_P due to the allocation trade-off (see appendix A) and the plant and pollinator densities at equilibrium (eq 3, main text). The relative fitness function of a mutant plant with attractiveness α_m compared to a resident plant with attractiveness α is:

$$\omega(\alpha_m,\alpha)=\frac{1}{P_m}\frac{dP_m}{dt}\bigg|_{P_m\to 0}=r_P(\alpha_m)-c_P P^*(\alpha)+\alpha_m \gamma_A A^*(\alpha), \tag{B3}$$

with P_m the mutant population density. As explained in the main manuscript, evolutionary endpoints (also called singular strategies) are obtained when trait variation goes to zero. Trait variations are given by the Canonical equation, into which lies the selection gradient (main text, equation (5). Its sign will give the direction of the trait evolution. Here the selection gradient corresponds to slope of the fitness function (B3) at the resident trait α, given a small variation in the trait (α_m).

$$\frac{\partial\omega(\alpha_m,\alpha)}{\partial\alpha_m}=\frac{dr_P(\alpha_m)}{d\alpha_m}+\gamma_A A^*(\alpha), \tag{B4}$$

Because of the hypothesis of small mutations, this yields:

$$\left.\frac{\partial \omega(\alpha_m,\alpha)}{\partial \alpha_m}\right|_{\alpha_m \to \alpha} = \left.\frac{d r_P(\alpha_m)}{d \alpha_m}\right|_{\alpha_m \to \alpha} + \gamma_A A^*(\alpha), \tag{B5}$$

Because all other terms of the Canonical Equation (5) are positive, the evolutionary singular strategy ($\hat{\alpha}$) is found using:

$$\left.\frac{\partial \omega(\alpha_m,\alpha)}{\partial \alpha_m}\right|_{\alpha_m,\alpha \to \hat{\alpha}} = \left.\frac{d r_P(\alpha_m)}{d \alpha_m}\right|_{\alpha_m,\alpha \to \hat{\alpha}} + \gamma_A A^*(\hat{\alpha}) = 0, \tag{B6}$$

with $r_P(\alpha)$ defined in annex A by equation (A1) and A^* by equation (3) in the main article. This means that a singularity is obtained only when costs in terms of energy of alternative means of reproduction ($\left.\frac{\partial r_P(\alpha_m)}{\partial \alpha_m}\right|_{\alpha_m,\alpha \to \hat{\alpha}}$) match the benefits in terms of pollination when changing attractiveness ($\gamma_A A^*(\hat{\alpha})$).

Replacing r_P , we obtain:

$$\left.\frac{\partial \omega(\alpha_m,\alpha)}{\partial \alpha_m}\right|_{\alpha_m,\alpha \to \hat{\alpha}} = \frac{-\left(\frac{\hat{\alpha}}{\alpha_{max}}\right)^s \left(1-\left(\frac{\hat{\alpha}}{\alpha_{max}}\right)^s\right)^{\frac{1}{s}-1}}{\hat{\alpha}} + \gamma_A \frac{\hat{\alpha}\gamma_P r_P(\hat{\alpha}) + c_P r_A}{\alpha_N \alpha_P - \hat{\epsilon}^2 \gamma_N \gamma_P} = 0, \tag{B7}$$

In the linear case (i.e. when $s=1$), the singular strategy formula is:

$$\hat{\alpha} = \frac{c_P(c_A - \alpha_{max}\gamma_A r_A)}{\alpha_{max}\gamma_A \gamma_P} \tag{B8}$$

This solution is feasible (i.e. positive and in a plausible range value), with $\alpha_{max} < \alpha_{cl}$ as defined in equation (4) of the main text, if and only if $0 < c_A < \alpha_{max}\gamma_A r_A$; i.e. the intraspecific competitive losses need to stay below the maximal energetic gain of the animal.

Conditions for invasibility

With the trade-off function defined in appendix (A1) we can differentiate the fitness function a second time to analyse the convergence and invasibility of the singular strategies, in order to deduce the overall trait dynamics [3]. The singular strategy ($\hat{\alpha}$) is non-invasible (ie, an ESS [4]) when:

$$\left.\frac{\partial \omega^2(\alpha_m,\alpha)}{(\partial \alpha_m)^2}\right|_{\alpha_m,\alpha \to \hat{\alpha}} = \frac{(1-s)\left(\frac{\hat{\alpha}}{\alpha_{max}}\right)^s \left(1-\left(\frac{\hat{\alpha}}{\alpha_{max}}\right)^s\right)^{\frac{1}{s}-2}}{\hat{\alpha}^2} < 0 \tag{B9}$$

Concave trade-offs ($s>1$) therefore lead to non-invasible singular strategies, while convex trade-offs ($s<1$) yield invasible strategies.

In the case of a linear trade-off equation B9 is equal to 0, the strategy is neutral from an invasibility point of view.

Conditions for convergence

The previous equation, summed with the crossed derivation of the fitness function gives conditions for convergence of the singular strategy [3]. The singular strategy is convergent when:

$$\left.\frac{\partial \omega^2(\alpha_m,\alpha)}{(\partial \alpha_m)^2}\right|_{\alpha_m,\alpha\to\hat{\alpha}} + \left.\frac{\partial \omega^2(\alpha_m,\alpha)}{\partial \alpha \partial \alpha_m}\right|_{\alpha_m,\alpha\to\hat{\alpha}} < 0 \qquad \text{(B10)}$$

The above mentioned formula requires the calculation of the cross-derivation. Using results from equation B6, it gives:

$$\left.\frac{\partial \omega^2(\alpha_m,\alpha)}{\partial \alpha \partial \alpha_m}\right|_{\alpha_m,\alpha\to\hat{\alpha}} = \gamma_A \frac{d A^*(\hat{\alpha})}{d\alpha} \qquad \text{(B11)}$$

According to the formula of $A^*(\hat{\alpha})$ given in equation (3) of the main article, the previous equation is equivalent to:

$$\left.\frac{\partial \omega^2(\alpha_m,\alpha)}{\partial \alpha \partial \alpha_m}\right|_{\alpha_m,\alpha\to\hat{\alpha}} = \frac{\gamma_A \gamma_P (2 c_P \gamma_A r_A + (c_A c_P + \hat{\alpha}^2 \gamma_A \gamma_P) r_P(\hat{\alpha}) + \hat{\alpha}(c_A c_P - \hat{\alpha}^2 \gamma_A \gamma_P) r_P'(\hat{\alpha}))}{(c_A c_P - \alpha^2 \gamma_A \gamma_P)^2} \qquad \text{(B12)}$$

with $r_P(\hat{\alpha})$ defined in annex A by equation (A1), and $r_P'(\hat{\alpha}) = r_P(\hat{\alpha}) \frac{1}{\hat{\alpha} - \left(\frac{\hat{\alpha}}{\alpha_{max}}\right)^{-s}}$

The sum of equation B12 at the eco-evolutionary equilibrium (i.e. when $\alpha_{max}, \alpha \to \hat{\alpha}$) and B9 is however too complex in the general case to give a simple to understand the convergence condition (as required by equation B10)

In the linear case (i.e. when $s=1$), equation B12 at the eco-evolutionary equilibrium becomes:

$$\left.\frac{\partial \omega^2(\alpha_m,\alpha)}{\partial \alpha \partial \alpha_m}\right|_{\alpha_m,\alpha\to\hat{\alpha}} = \frac{\gamma_A \gamma_P \left(c_A c_P + \hat{\alpha}^2 \gamma_A \gamma_P + 2 c_P \hat{\alpha} \left(\gamma_A r_A - \frac{c_A}{\alpha_{max}}\right)\right)}{(c_A c_P - \hat{\alpha}^2 \gamma_A \gamma_P)^2} \qquad \text{(B13)}$$

Because $\left.\frac{\partial \omega^2(\alpha_m,\alpha)}{(\partial \alpha_m)^2}\right|_{\alpha_m,\alpha\to\hat{\alpha}} = 0$, the convergence condition then depends only on the above cross derivation B13.

replacing $\hat{\alpha}$ by the expression from equation B8 gives:

$$\left.\frac{\partial \omega^2(\alpha_m,\alpha)}{\partial \alpha \partial \alpha_m}\right|_{\alpha_m,\alpha\to\hat{\alpha}} = \frac{-\gamma_A^2 \gamma_P^2 \alpha_{max}^2}{c_P\left(c_A^2 c_P + c_P \gamma_A^2 r_A^2 \alpha_{max}^2 - c_A \gamma_A \alpha_{max}\left(2 c_P r_A + \gamma_P \alpha_{max}\right)\right)} \tag{B14}$$

With conditions on the parameter values (i.e. all parameter values are positives, ratesvalues stay below 1 and $\alpha_{max} < \alpha_{cl}$) the above derivation is always positive, meaning that a linear trade-off always leads to a divergent singular strategy.

References

1. Willmer P. 2011 Rewards and costs: the environmental economics of pollination. In *Pollination and Floral Ecology*, pp. 234–257. Princeton University Press.

2. Handel SN. 1985 The Intrusion of Clonal Growth Patterns on Plant Breeding Systems. *Am. Nat.* **125**, 367–384. (doi:10.1086/284348)

3. Dieckmann U, Law R. 1996 The dynamical theory of coevolution: a derivation from stochastic ecological processes. *J. Math. Biol.* **34**, 579–612. (doi:10.1007/BF02409751)

4. Maynard Smith J. 1982 *Evolution and the Theory of Games*. Cambridge University Press.